

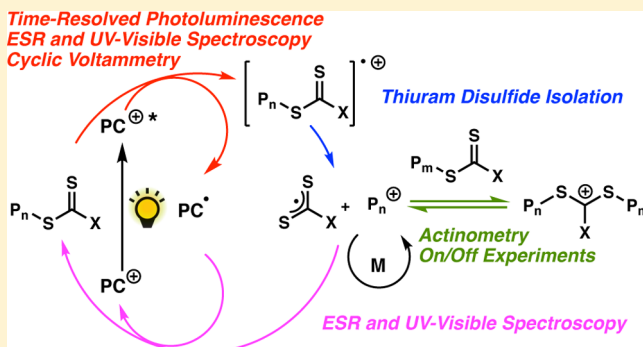
# Mechanistic Insight into the Photocontrolled Cationic Polymerization of Vinyl Ethers

Quentin Michaudel, Timothée Chauviré,<sup>1</sup> Veronika Kottisch, Michael J. Supej, Katherine J. Stawiasz, Luxi Shen, Warren R. Zipfel, Héctor D. Abruña,<sup>2</sup> Jack H. Freed,<sup>3</sup> and Brett P. Fors<sup>1\*</sup>

Cornell University, Ithaca, New York 14853, United States

## Supporting Information

**ABSTRACT:** The mechanism of the recently reported photocontrolled cationic polymerization of vinyl ethers was investigated using a variety of catalysts and chain-transfer agents (CTAs) as well as diverse spectroscopic and electrochemical analytical techniques. Our study revealed a complex activation step characterized by one-electron oxidation of the CTA. This oxidation is followed by mesolytic cleavage of the resulting radical cation species, which leads to the generation of a reactive cation—this species initiates the polymerization of the vinyl ether monomer—and a dithiocarbamate radical that is likely in equilibrium with the corresponding thiuram disulfide dimer. Reversible addition–fragmentation type degenerative chain transfer contributes to the narrow dispersities and control over chain growth observed under these conditions. Finally, the deactivation step is contingent upon the oxidation of the reduced photocatalyst by the dithiocarbamate radical concomitant with the production of a dithiocarbamate anion that caps the polymer chain end. The fine-tuning of the electronic properties and redox potentials of the photocatalyst in both the excited and the ground states is necessary to obtain a photocontrolled system rather than simply a photoinitiated system. The elucidation of the elementary steps of this process will aid the design of new catalytic systems and their real-world applications.



## INTRODUCTION

The wealth of photoredox reactions developed during the past decade has offered a blank canvas on which to design “living” polymerizations in which polymer chain growth can be controlled at will by the intensity or wavelength of light.<sup>1</sup> The intrinsic resolution of light enables unparalleled spatial control over these polymerizations, a factor that may prove desirable in a wide array of settings. Photocontrolled variants of living radical polymerizations, including atom-transfer radical polymerization (ATRP),<sup>2</sup> organotellurium-mediated radical polymerizations (TERP),<sup>3</sup> and reversible addition–fragmentation chain transfer (RAFT) polymerizations,<sup>4</sup> have already demonstrated usefulness with a variety of monomers. This unprecedented command over polymeric architectures inspires numerous applications from the complex patterning of surfaces<sup>5</sup> to the synthesis of sequence-controlled polymers.<sup>6</sup>

In an effort to expand the range of monomers capable of light-regulated polymerization, we recently reported a photocontrolled cationic polymerization of vinyl ethers.<sup>7</sup> As shown in Figure 1, our initial reaction conditions capitalized on the high potency of the oxidative photocatalyst (PC) 2,4,6-tris(4-methoxyphenyl)pyrylium tetrafluoroborate (**1a**) when combined with chain-transfer agents (CTAs) **2a** or **2b** as a means to control the cationic polymerization of various vinyl ethers (**3a–e**). Polymers with predictable number-average molar mass ( $M_n$ )

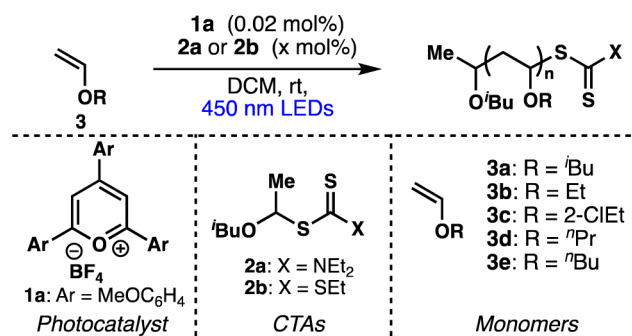


**Figure 1.** Cationic polymerization of vinyl ethers regulated with blue light.

and narrow dispersity ( $\mathcal{D}$ ) values were obtained by modulating the CTA-to-monomer ratio. These conditions reversibly generate cationic chain ends that propagate in the presence of light and are deactivated in the dark, thus enabling the temporal regulation of chain growth through light irradiation. In contrast to previously reported radical systems that rely on the chain end reduction, this cationic process requires oxidation of the terminal

**Received:** September 6, 2017

**Published:** October 6, 2017

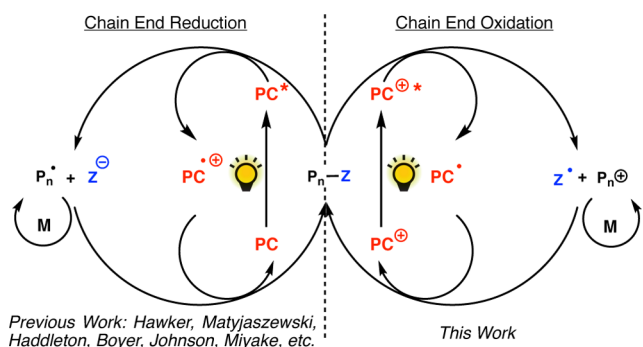


**Figure 2.** Photocontrolled radical polymerization vs cationic polymerization: two mechanistically distinct pathways. PC = photocatalyst; Z = Br,  $S_2CR$ ,  $S_2CSR'$ , etc.

group (Figure 2), which suggests that the transformation proceeds through a mechanistic pathway that is fundamentally distinct from those of its radical counterparts. A deeper understanding of the mechanism of this unique polymerization is critical for applications to a broader range of monomers and, more important, the design of more intricate systems.

Our current mechanistic hypothesis is depicted in Figure 3. Single-electron transfer (SET) from the CTA (or polymer chain

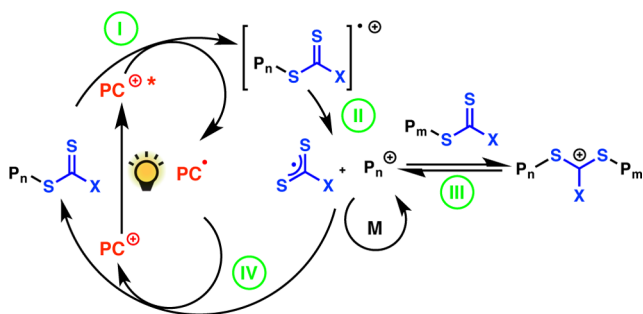


**Figure 3.** Proposed mechanism for the light-regulated polymerization of vinyl ethers via a photocatalyst (PC) and chain-transfer agent.

end) to the excited PC generates a radical cation species (step I) that undergoes mesolytic cleavage, leading to the formation of an active cationic chain end and a stable dithiocarbamate or trithiocarbonate radical (step II). The resulting cationic species is then engaged in a RAFT-type degenerative chain transfer (step III). Finally, one-electron reduction of the stable radical by  $PC^{\bullet}$  turns over the PC while producing a dithiocarbamate (or trithiocarbonate) anion, which caps the polymer chain end and deactivates chain growth (step IV).

To probe the elementary steps, we used a combination of spectroscopies—namely, time-resolved photoluminescence, UV–visible absorption, and electron spin resonance (ESR)—and electrochemistry. The efficiencies of the polymerization were also explored with a number of PCs and CTAs. The body of data presented herein reveals much about the processes at play and should serve as a platform for the development of related transformations and translational technologies.

## RESULTS AND DISCUSSION

**Exploration of the Photocatalytic System.** Building on our initial report, we investigated several factors that could influence the polymerization kinetics and control in these systems, such as the choice of PC, CTA, and solvent. All reactions

were kept at ambient temperature under a constant stream of air and placed at a fixed distance from the light. Isobutyl vinyl ether (IBVE, 3a) was used as a reference monomer.

**Influence of PCs on Polymerization Rates.** Our mechanistic hypothesis states that the rates of activation (step I) and deactivation (step IV) for a given CTA should be governed primarily by the nature of the PC. In an attempt to pinpoint the key features of an efficient PC for this system, we prepared an array of pyrylium derivatives (1a–e; Figure 4; see Supporting

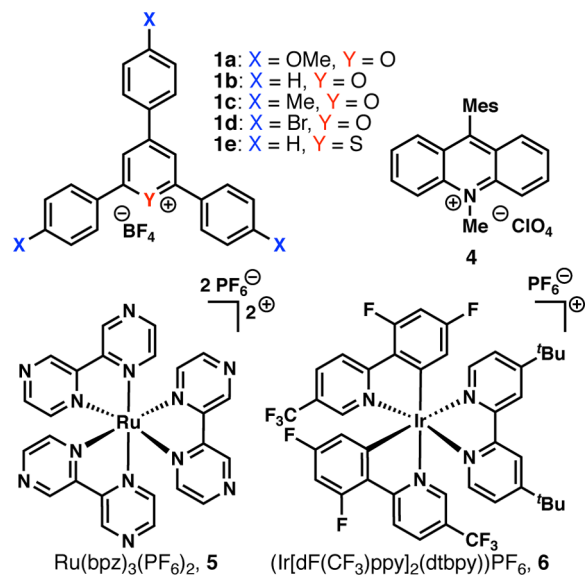


**Figure 4.** Photocatalysts used for the study.

Information [SI] for details).<sup>8–11</sup> The para substituent of each aryl group as well as the heteroatom of the pyrylium core are easily tuned through synthesis, which allows for simple modulation of the redox and photophysical properties of the catalyst (Table 1). Other strongly oxidizing photoredox catalysts were used for this study as well, including acridinium 4 and ruthenium or iridium complexes 5 and 6.<sup>12–17</sup>

**Table 1. Redox Potentials and Photophysical Properties of Photocatalysts**

PC	$E_{PC^{\bullet+}/PC^{\bullet}}$ (V vs SCE)	$E_{PC^{\bullet+}/PC^{\bullet}}$ (V vs SCE)	$\epsilon_{450}$ (L·mol <sup>-1</sup> ·cm <sup>-1</sup> )	$\Phi_f$	$\Phi_{ISC}$
1a	+1.84 <sup>a,8</sup>	−0.50 <sup>8</sup>	67 300 <sup>b</sup>	0.95 <sup>8</sup>	0.03 <sup>8</sup>
1b	+2.55 <sup>a,8</sup>	−0.32 <sup>8</sup>	6350 <sup>b</sup>	0.58 <sup>8</sup>	0.42 <sup>8</sup>
1c	+2.23 <sup>9</sup>	−0.55 <sup>9</sup>	32 100 <sup>b</sup>	—	—
1d	+2.49 <sup>10</sup>	−0.03 <sup>10</sup>	30 100 <sup>b</sup>	0.33 <sup>11</sup>	0.67 <sup>11</sup>
1e	+2.45 <sup>a,8</sup>	−0.19 <sup>8</sup>	7330 <sup>b</sup>	0.03 <sup>8</sup>	0.94 <sup>8</sup>
4	+2.18 <sup>a,8</sup>	−0.49 <sup>8</sup>	4030 <sup>12</sup>	0.035 <sup>8</sup>	0.38 <sup>8</sup>
5	+1.45 <sup>13</sup>	−0.80 <sup>13</sup>	9000 <sup>14</sup>	0.034 <sup>15</sup>	0.68 <sup>15</sup>
6	+1.21 <sup>13</sup>	−1.37 <sup>13</sup>	1760 <sup>16</sup>	0.68 <sup>16</sup>	—

<sup>a</sup>Potential of the singlet excited state. <sup>b</sup>Experimentally determined in dichloromethane (see Supporting Information). Reference numbers for each reported physical data are indicated.

The results from the polymerization of 3a using CTA 2a, a PC, and blue LEDs are summarized in Table 2. Notably, only pyrylium derivatives afforded polymers (Table 2, entries 1–7), all of which had  $M_n$ 's close to theoretical values and  $D$ 's of approximately 1.2. In the dark, no polymerization was observed (Table 2, entry 11).<sup>7</sup> Phenyl and tolyl derivatives 1b and 1c

**Table 2. Selected Results of Cationic Polymerization of Isobutyl Vinyl Ether (3a) with Various Photocatalysts**

entry <sup>a</sup>	catalyst	time (min)	$M_n$ (exp) (kg/mol)	$M_n$ (theo) (kg/mol) <sup>f</sup>	$\bar{D}$
1	1a	480	10.7	10.1	1.19
2	1b	10	10.5	10.1	1.23
3	1b <sup>b</sup>	10	10.2	10.1	1.19
4	1c	10	11.1	10.1	1.17
5	1c <sup>b</sup>	30	10.7	10.1	1.17
6	1d	480	10.5	10.1	1.18
7	1e	300	10.3	10.1	1.21
8	4	— <sup>c</sup>	—	10.1	—
9	5	— <sup>c</sup>	—	10.1	—
10	6	— <sup>c</sup>	—	10.1	—
11	1a <sup>d</sup>	— <sup>c</sup>	—	10.1	—

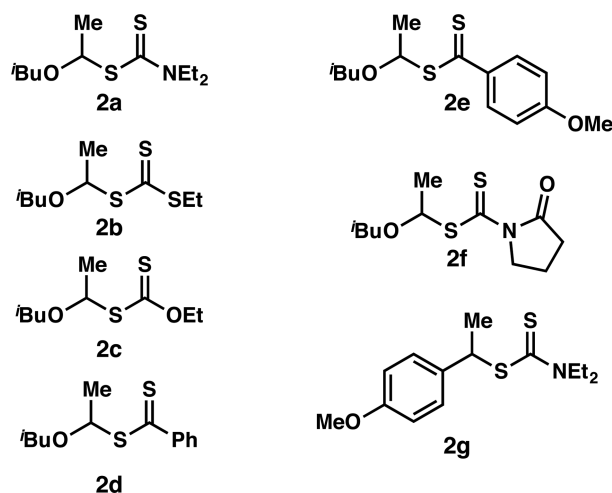
<sup>a</sup>Reaction conditions: 3a (1 equiv), photocatalyst (PC; 0.02 mol %), and 2a (0.01 equiv) at room temperature in dichloromethane with blue-light-emitting diode irradiation (9 W bulb). <sup>b</sup>Using 0.01 mol % of PC. <sup>c</sup>No irradiation. <sup>d</sup>No conversion was observed after 720 min. <sup>f</sup>Conversion was determined by <sup>1</sup>H NMR using benzene as an internal standard.

(Table 2, entries 2–5) demonstrated the highest polymerization rates, reaching full conversion after less than 10 min compared with several hours for 1a. This outcome is likely due to the higher oxidation potentials of the PCs ( $E^\circ_{1b^*/1b^*} = +2.55$  V and  $E^\circ_{1c^*/1c^*} = +2.23$  V, whereas  $E^\circ_{1a^*/1a^*} = +1.84$  V vs SCE). The relatively slower rate observed with thiopyrylium 1e compared with that of 1b despite the similar redox potentials and molar attenuation coefficients of these compounds may be linked to a low quantum yield of fluorescence ( $\Phi_f = 0.03$ ), which implies that the singlet excited state of the pyrylium contributes mainly to the electron transfer step. However, additional experiments are required to confirm the exact role of both the singlet and the triplet states in this reaction.<sup>18</sup> Finally, the lower reactivity of tribromo congener 1d compared with that of the other pyryliums is likely due to poor solubility in dichloromethane (Table 2, entry 6).

**Influence of the CTA on Chain Growth Control.** Because 2a and 2b play the dual role of initiator and CTA, we hypothesized that the structure of the CTA may profoundly affect the photocontrol of the process.<sup>19</sup> We therefore synthesized a library of CTAs (2c–f) with various groups appended to the dithiocarboxylic core. We also synthesized one CTA (2g) prepared from 4-methoxystyrene rather than IBVE (Figure 5). We anticipated that xanthate 2c, dithioesters 2d and 2e, and pyrrolidinone dithiocarbamate 2f would show electronic properties distinct from those of 2a and 2b, a factor that should impact the rate of each step in the mechanism.

In our previous study,<sup>7</sup> we found that, compared with 2a, CTA 2b was applicable to a wider monomer scope and delivered polymers with only a slightly broader  $\bar{D}$ . However, the preparation of 2a with greater purity enabled the controlled polymerization of ethyl vinyl ether (EVE; Table 3, entry 2), *n*-propyl vinyl ether, and *n*-butyl vinyl ether (see SI). Polymerization attempts with 2-chloroethyl vinyl ether and 2a resulted in no conversion (see SI), and 2b is still required for this monomer. Consequently, the purity of the CTA is paramount to the polymerization of less reactive monomers.

The polymerization of IBVE (3a) or EVE (3b) using CTAs 2c, 2d, and 2f yielded macromolecules with  $M_n$ 's mostly in agreement with theoretical calculations but with broader  $\bar{D}$ 's ( $1.9 < \bar{D} < 2.2$ ; Table 3, entries 5–8 and 11–12). The experimental  $M_n$ 's of xanthate 2c and dithioester 2d were higher

**Figure 5.** Library of chain-transfer agents used for this study.**Table 3. Selected Results of the Cationic Polymerization of Isobutyl Vinyl Ether (3a) and Ethyl Vinyl Ether (3b) with Various Chain-Transfer Agents**

entry <sup>a</sup>	CTA	monomer	$M_n$ (exp) (kg/mol)	$M_n$ (theo) <sup>b</sup> (kg/mol)	$\bar{D}$
1	2a	3a	9.11	10.1	1.16
2	2a	3b	7.39	7.3	1.12
3	2b	3a	10.1	10.1	1.43
4	2b	3b	8.20	7.3	1.35
5	2c	3a	15.1	10.1	1.98
6	2c	3b	10.6	7.3	1.89
7	2d	3a	15.0	10.1	2.10
8	2d	3b	10.9	7.3	2.11
9	2e	3a	9.43	10.1	1.49
10	2e	3b	7.23	7.3	1.47
11	2f	3a	12.9	10.1	2.18
12	2f	3b	10.4	7.3	2.21
13	2g	3a	74.9	10.1	3.76
14	2g	3b	40.5	7.3	3.18
15	—	3a	52.2	—	3.96

<sup>a</sup>Reaction conditions: 3a (1 equiv), 1a (0.01 mol %), and chain-transfer agent (0.02 equiv) at room temperature in dichloromethane with blue-light-emitting diode irradiation (ca. 12 W LED strip) for 360 min. <sup>b</sup>Conversion was determined by <sup>1</sup>H NMR using benzene as an internal standard.

than predicted with both monomers (Table 3, entries 5–8). By contrast, CTA 2e enabled control similar to that offered by 2b (Table 3, entries 9 and 10). Subtle increase of the electron donating character of the aryl group therefore has a crucial effect on the control over the chain growth. The CTA derived from 4-methoxystyrene (2g) resulted in uncontrolled polymerization with both monomers (Table 3, entries 13 and 14), which indicates that the monothioacetal structure is critical. Notably, uncontrolled polymerization occurs in the absence of CTA (Table 3, entry 15), which suggests that the direct activation of the monomer is a possible background pathway. Based on the aforementioned results, electron-rich X groups (see Figures 1 and 3 for the notation) such as nitrogen- and sulfur-containing moieties should be favored in the design of future CTAs. Moreover, only CTAs derived from vinyl ethers exhibited good control over chain growth.

**Suitable Solvents for the Polymerization.**<sup>20</sup> Pyrylium salts have poor solubility in hydrocarbon solvents; therefore, benzene, toluene, and small alkanes are unsuitable for this methodology. Similarly, the high oxidizing strength of excited pyryliums precludes the use of solvents such as tetrahydrofuran (THF). Polymerizations in acetonitrile yielded well-controlled polymers, but poly(IBVE) started to phase-separate at an  $M_n$  of  $\sim 5$  kg/mol. A mixture of dichloromethane and acetonitrile prevented this issue. Last, almost no polymerization was observed in nitromethane, an outcome that agrees with the reported low propagation rates of cationic polymerization of vinyl ethers in this solvent.<sup>21</sup>

**Initial One-Electron Oxidation, a Critical Step for Activation.** The elucidation of the electron transfers among species in solution is key to understanding the activation of the cationic process (step I). Our previous studies revealed that the fluorescence of **1a**\* in a steady-state experiment is quenched by both CTA **2a** and IBVE (**3a**).<sup>7</sup> However, this result does not distinguish between static and dynamic quenching (Figure 6),

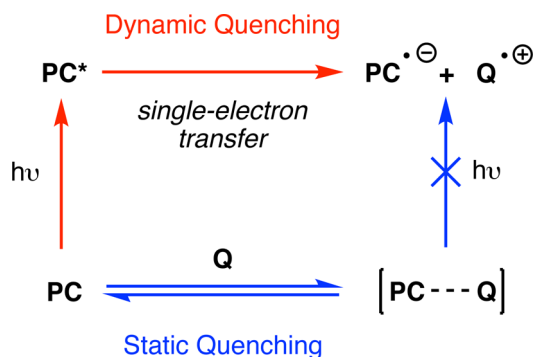


**Figure 6.** Static vs dynamic quenching of a photocatalyst (PC) by a quencher (Q).

and the latter is the only quenching at play for an electron transfer.<sup>22</sup> Therefore, time-resolved fluorescence spectroscopy was used in conjunction with ESR and electrochemical analysis to analyze electron transfer in these reactions.

**Time-Resolved Fluorescence Spectroscopy.** The fluorescence decay for PC **1a** using 440 nm pulsed excitation was measured with various amounts of potential quenchers, CTA **2a**, and monomer **3a** (Figures 7, 8, and S14). A clear decrease in the PC\* lifetime ( $\tau$ ) was observed with increasing concentrations of both **2a** and **3a**. More precisely, the relationship between  $\tau$  and the concentration of both quenchers (Figure 8) follows eq 1, which is directly derived from the Stern–Volmer equation, where  $\tau_0$  is the fluorescence lifetime of catalyst without quencher,  $k_q$  is the bimolecular quenching constant, and  $[Q]$  is the concentration of quencher.<sup>22</sup>

$$\frac{\tau_0}{\tau} = 1 + k_q \tau_0 [Q] \quad (1)$$

This behavior is consistent with collisional quenching occurring with both the CTA and the monomer. However, calculations of bimolecular quenching constants ( $k_q$ 's) suggest that the former is a more efficient quencher ( $k_q = 7.52 \times 10^9 \text{ M}^{-1} \cdot \text{s}^{-1}$ ) than **3a** ( $k_q = 1.23 \times 10^8 \text{ M}^{-1} \cdot \text{s}^{-1}$ ) by nearly 2 orders of magnitude. The quenching rate of CTA **2a** is near  $10^{10} \text{ M}^{-1} \cdot \text{s}^{-1}$ , which is characteristic of a diffusion-controlled process.<sup>22</sup> These observations suggest that SET can indeed occur between the singlet excited PC and either the CTA or the monomer. Transfer

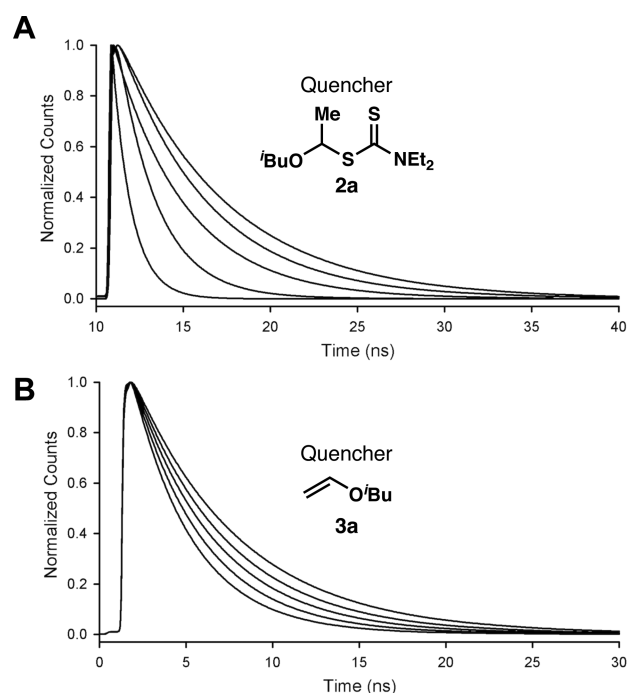


**Figure 7.** Fluorescence decay of **1a** after a 440 nm pulsed excitation: (A) For various concentrations of chain-transfer agent **2a**. (B) For various concentrations of isobutyl vinyl ether (**3a**).

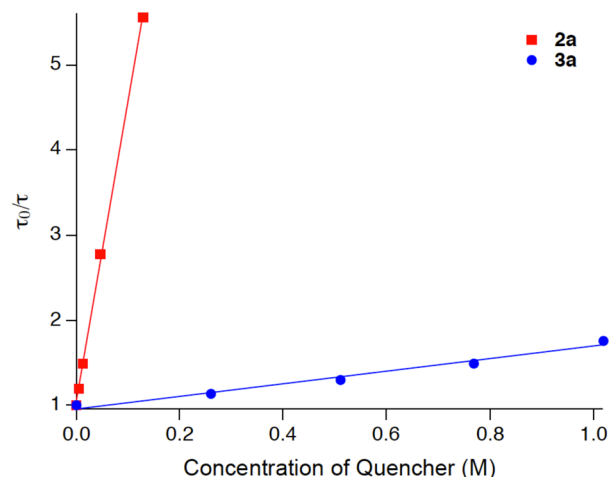


**Figure 8.** Linear relationship between the fluorescence lifetime of photocatalyst **1a** and the concentrations of **2a** (red) and **3a** (blue).

to the CTA is the more favorable pathway ( $k_q = 7.52 \times 10^9 \text{ M}^{-1} \cdot \text{s}^{-1}$ ); however, in the early stages of polymerization, the direct oxidation of the highly concentrated IBVE is feasible (Table 3, entry 15).

**Electropolymerization of IBVE.** The spectroscopic evidence discussed above agrees with the measured potentials corresponding to the onset of oxidation of both CTA **2a** ( $E^\circ_{2a/2a^{•+}} = +0.98 \text{ V}$  vs  $\text{Ag}/\text{Ag}^+$  [ $+1.19 \text{ V}$  vs SCE]) and **3a** ( $E^\circ_{3a/3a^{•+}} = +1.25 \text{ V}$  vs  $\text{Ag}/\text{Ag}^+$  [ $+1.46 \text{ V}$  vs SCE]) (Figure 9), the latter being more difficult to oxidize. Nevertheless, the oxidation of **3a** could potentially lead to uncontrolled polymerization, as seen when no CTA is added (Table 3, entry 15).<sup>23</sup> The absence of this background reaction when a CTA is used and at low PC loading can be rationalized by several electronic considerations. First, compared to **3a**, CTA **2a** is oxidized more readily by catalysts **1**. Second, if



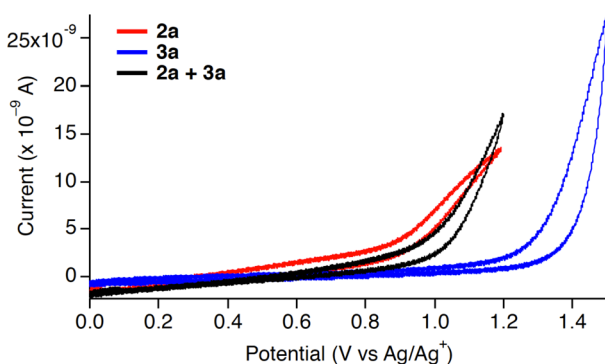


**Figure 9.** Cyclic voltammogram of **2a** (red), **3a** (blue), and a combination of **2a** and **3a** (black) using a platinum microelectrode (12.5  $\mu\text{m}$ ).

the oxidation of **3a** still occurs, the 270 mV difference in potentials should allow for a second electron transfer from oxidized **3a** to CTA **2a**.

To assess whether the direct oxidation of CTA **2a** leads to polymerization, we obtained a cyclic voltammogram of **3a** with and without **2a** (Figure 9). The absence of a reduction wave in both cases likely reflects the irreversibility of the reaction and, potentially, the passivation at the electrode due to the growth of poly(IBVE). Compared to IBVE alone, the onset of oxidation with **2a** lies ca. 300 mV lower, which suggests that the polymerization of **3a** can be effected at a lower potential (ca. +0.8 V vs Ag/Ag<sup>+</sup>) when CTA **2a** is present. Indeed, the polymerization of **3a** could be initiated at an applied voltage of +0.8 V vs Ag/Ag<sup>+</sup> in the presence of **2a** (see SI), whereas no polymer was isolated in the absence of **2a** under the same conditions. This result supports the conclusion that the direct oxidation of CTA **2a** is the major pathway for step I and that a two-step oxidation via an oxidized monomer species is likely only a minor concurrent pathway.

**ESR and UV–visible Characterization of Pyranil Radicals 1a• and 1b•.** ESR spectroscopy has proven to be a powerful tool for the observation of free radical species in similar polymerization systems;<sup>18,24</sup> moreover, both **1a•** and **1b•** have previously been characterized using this technique,<sup>25,26</sup> which prompted the use of ESR as a means to track our postulated electron transfers. Samples containing a mixture of CTA **2a** and PCs **1a** or **1b** were monitored during steady-state irradiation with blue LEDs. The beginning of irradiation coincided with the appearance of an ESR absorption signal with both PCs (Figure 10), an observation characteristic of stable radical intermediates. With the combination of **1b** and **2a**, a hyperfine splitting structure was observed, which was expected due to the numerous aromatic protons adorning the pyrylium core. This hyperfine coupling (hfc) structure could be reproduced through simulation (Figure S15A) and was in complete agreement with previously reported hfc constants for that compound.<sup>25</sup> Moreover, the formation of **1b•** was confirmed with UV–visible absorption spectroscopy (Figure S21A).<sup>25b</sup> By contrast, no hyperfine splitting structure was observed for the analogous system containing **1a** and **2a**, even when a low-amplitude modulation was used ( $M = 0.08$  G).<sup>27</sup> However, this absence of hyperfine structure was noted by Kawata and colleagues<sup>26</sup> and could be due to a broadening induced by the Heisenberg exchange effect.<sup>28</sup> To unambiguously attribute the signal arising from the irradiation of **1a** and CTA **2a** to pyranil radical **1a•**, we used THF, a known sacrificial electron donor,<sup>25,26</sup> in lieu of CTA **2a** (Figure S16). A comparison of

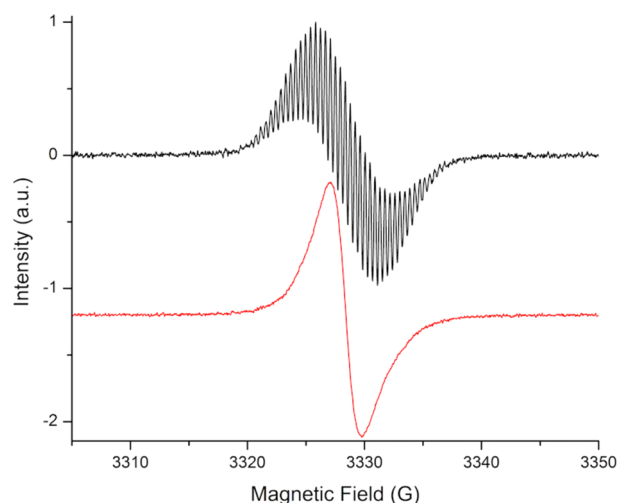


**Figure 10.** Electron spin resonance spectrum of **1a** with **2a** (red) and **1b** with **2a** (black) under steady-state 450 nm irradiation.

these results with the spectrum in Figure 10 corroborates the suggested formation of pyranil radical **2a** in the reaction conditions.

Having confirmed the one-electron oxidation of CTA **2a** by excited PCs **1a** or **1b**, we turned our attention to the putative electron transfer between **1a** (or **1b**) and vinyl ether **3a**. Steady-state irradiation of a mixture of **1a** and **3a** or **1b** and **3a** revealed the formation of a long-lived radical species (Figure 11). A

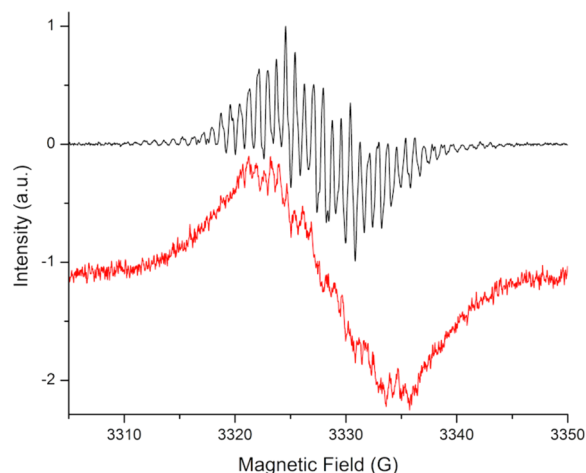


**Figure 11.** Electron spin resonance spectrum of **1a** with IBVE (**3a**; red) and **1b** with **3a** (black) under steady-state 450 nm irradiation.

comparison of these results to the traces in Figure 10 revealed striking differences. In particular, these new radical species have broader signals and different hyperfine splitting structures. Furthermore, the ESR spectra showed a broadening of the line width over the course of the acquisition, which may be caused by the increase in viscosity during the polymerization.<sup>29</sup> Considered together, these results suggest that radical species other than **1a•** and **1b•** are created in the presence of **3a**. However, the complex hyperfine splitting structure of these new radical species indicates that the adducts contain a pyrylium core structure.

Several hypotheses may explain the discrepancies between the spectra in Figures 10 and 11. First, after the initial photoinduced electron transfer, radicals **1a•** or **1b•** may react with **3a** to generate a new adduct. Second, the high concentration of IBVE

may induce conformational change through noncovalent bonding, thereby leading to a nonequivalent set of hfc's via the loss of C2 symmetry. To distinguish between these possibilities, we added **3a** to a sample containing **1b**<sup>•</sup>, which was pregenerated using THF as an electron donor. No change was observed in either the hyperfine structure or the intensity of the signal after **3a** addition (Figure S20), which indicates that no reaction occurred between **1b**<sup>•</sup> and **3a**. Thus, we investigated the potential formation of a donor–acceptor complex between ground state **1a** (or **1b**) and the electron-rich monomer (**3a**). Equilibrium 1 illustrates this hypothesis in the case of **1a** (Figure 12).

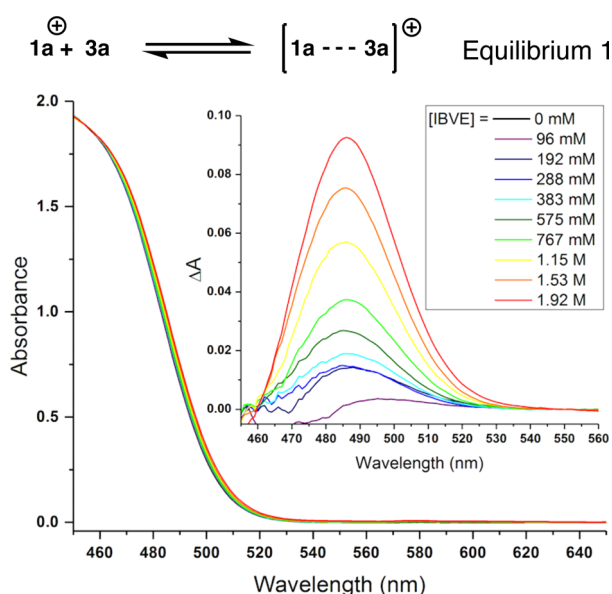


**Figure 12.** Formation of a donor–acceptor complex between **1a** and **3a**: UV–visible spectra of **1a** with various concentrations of **3a**.

The results of careful UV–visible absorption spectroscopy of **1a** and **1b** with various amounts of **3a** revealed a slight shift of the local absorption maximum above 450 nm (Figure 12). This new band at 487 nm was attributed to the absorption of  $[1 \cdots 3a]^+$ , and the equilibrium constants  $K_{DA}$  were estimated to be 0.06 M (for **1a**) and 0.19 M (for **1b**) according to the Benesi–Hildebrand method (Figure S22).<sup>30</sup> Nicewicz and co-workers have previously demonstrated the impact of similar donor–acceptor complexes on the dynamics of alkene oxidation by acridinium PCs,<sup>12</sup> and we expect that, similarly, the formation of  $[1 \cdots 3a]^+$  significantly influences the kinetics of electron transfer. Consistent with this finding, a spectrum that has good correlation with the experimental ESR signal in Figure 11 could be simulated by adding two equivalent protons to the spin system of **1b**<sup>•</sup> (Figure S19).<sup>31</sup> Finally, ESR analysis of the complete polymerization system—namely, **1a** (or **1b**), CTA **2a**, and monomer **3a**—produced spectra similar to those in Figure 11 (Figures S17 and S18).

**Exploration of the Mesolytic Cleavage.** The second key step of our mechanism involves the cleavage of the radical cation arising from CTA or chain end oxidation into a dithiocarbamate radical and a propagating cationic chain. Vinyl ethers are known to homopolymerize under cationic conditions, but the analogous process has not been observed under radical conditions,<sup>32</sup> which substantiates the fragmentation pattern described above. Furthermore, when methyl methacrylate was added to the

polymerization mixture, no poly(methyl methacrylate), a product expected from alkyl radical formation, was isolated.<sup>33</sup>

Significantly, when blue light was shone on the reaction of CTA **2a** and catalyst **1a** in a ratio typical of the polymerization, the only isolated products were thiuram disulfide **7** and starting material **2a** (see Figure 13A and SI). Compound **7** likely arises

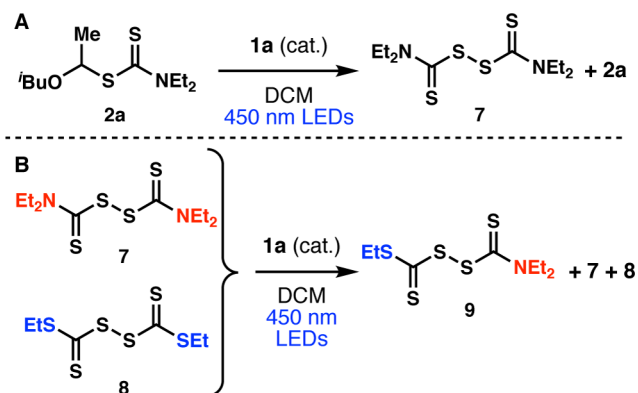


**Figure 13.** (A) Isolation of thiuram disulfide **7** via putative mesolytic cleavage. (B) Crossover experiment with disulfides **7** and **8**.

from radical recombination after mesolytic cleavage. Indeed, one-electron oxidation of sodium dithiocarbamate affords thiuram disulfide **7** in excellent yields with various oxidants such as iodine (see SI).<sup>34</sup>

Thiuram disulfides are commonly used as CTAs for radical RAFT polymerization and as reagents for the vulcanization of rubber.<sup>35</sup> Notably, when substituted for CTA **2a**, disulfide **7** affords no control over the polymerization (Table S7), a result that agrees with the proposed cationic process. Disulfide **7** was not detected during NMR analysis of aliquots obtained over the course of the polymerization reactions, which may be attributed to the detection limits of NMR spectroscopy or the rapidity of the reduction of the radical or disulfide dimer (step IV, *vide infra*). Moreover, a crossover experiment with disulfides **7** and **8** indicated that **7** is in equilibrium with the radical dithiocarbamate in the reaction conditions (Figure 13B), which agrees with the results of previous studies.<sup>12</sup>

**Is a RAFT Equilibrium Occurring?** In their initial report of a cationic RAFT process, both Kamigaito<sup>19b,36</sup> and Sugihara<sup>37</sup> invoked a degenerative chain transfer to account for the observed control over chain growth. However, from a mechanistic standpoint, our photoredox process differs in that CTA **2a** plays the role of both initiator and CTA, as shown by steps I, II, and IV. From this proposed catalytic cycle, it is unclear whether the RAFT equilibrium (step III) is truly necessary to achieve control over chain growth. Therefore, we devised experiments to ascertain the presence or absence of such equilibrium in this polymerization. Quantum yields of the polymerization were estimated through actinometry, and temporal control was investigated with PCs **1a** and **1b**.

**Quantum Yields of the Polymerization.** Using the well-studied potassium ferrioxalate actinometer (see SI, Figure S23, for more details),<sup>38</sup> the quantum yields of polymerization were estimated to be approximately 6 monomer additions per photon absorbed for PC **1a** (0.02 mol %) and approximately 35 monomer additions/photon for **1b** (0.01 mol %). This difference was anticipated based on the higher polymerization rate measured for **1b** compared with that of **1a** (Table 2). By contrast, photoinitiated cationic polymerizations are character-

ized by higher quantum yields such as 200 monomer additions/photon.<sup>39</sup> However, the fact that both quantum yields are well above unity suggests that a chain-degenerative mechanism, as shown in step III, is likely occurring, because narrow  $\bar{D}$ 's and predictable  $M_n$ 's were obtained for all pyrylium PCs.

**On/Off Experiments with PCs 1a and 1b.** The stark differences in polymerization rates and quantum yields between PCs 1a and 1b led us to investigate whether temporal control over chain growth is possible with the latter. A reaction mixture containing monomer 3a, catalyst 1a (or 1b), and CTA 2a was exposed to light and then stirred in the dark for the same time period and re-exposed to light (Figure 14). Conversion and  $M_n$

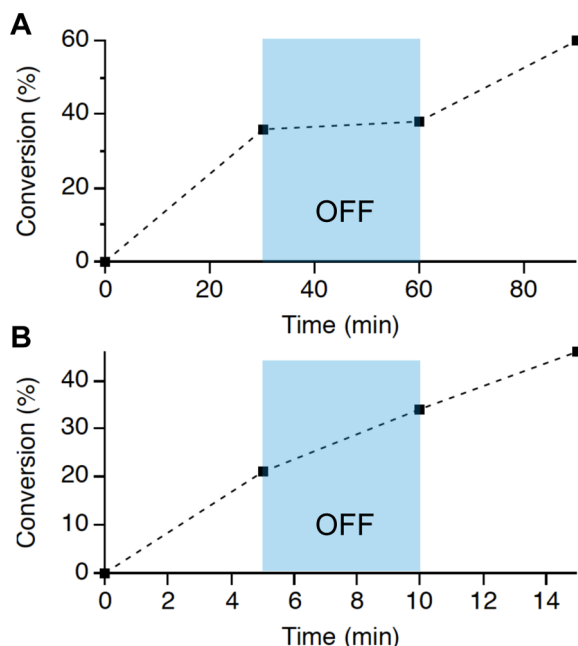


**Figure 14.** Monomer conversion vs time with intermittent light exposure with photocatalysts (A) 1a and (B) 1b.

were monitored at each switching point with NMR spectroscopy and size exclusion chromatography analyses of aliquots. Although the plot of conversion versus time clearly illustrates that polymerization proceeds only in the presence of light with 1a (Figure 14A), the corresponding plot for 1b shows that polymerization is not halted in the dark (Figure 14B). Consequently, pyrylium 1b should be considered a fine catalyst for photoinitiated, rather than photocontrolled, cationic polymerization,<sup>1f</sup> as it allows for predictable  $M_n$  and a  $\bar{D}$  of  $\sim 1.2$  but offers no temporal control of chain growth. This outcome also suggests that the recapping step (step IV) is much slower for 1b than for 1a, which can be explained by the difference in ground state redox potentials ( $E^\circ_{1a^+/1a^\bullet} = -0.50$  V versus SCE, and  $E^\circ_{1b^+/1b^\bullet} = -0.32$  V versus SCE).<sup>8</sup> Indeed, the redox potential for the reduction of disulfide 7 has been measured at  $E^\circ_{7/7^\bullet} = -0.302$  V versus SCE by Nichols and Grant,<sup>40</sup> which supports our conclusion that reduction of 7 is more likely with 1a $^\bullet$  than with 1b $^\bullet$ , therefore resulting in a more efficient deactivation of chain growth with the former. However, the fact that living characteristics are observed with both photocatalysts is a strong indicator that a RAFT equilibrium influences chain growth.

**Catalyst Turnover and Chain End Capping.** The last step of our proposed mechanism was interrogated via an ESR experiment coupled with UV–visible spectroscopy. The

reduction of 1a with a stoichiometric amount of cobaltocene (CoCp<sub>2</sub>)<sup>41</sup> afforded radical 1a $^\bullet$ , as shown in Figure 15 (see SI for

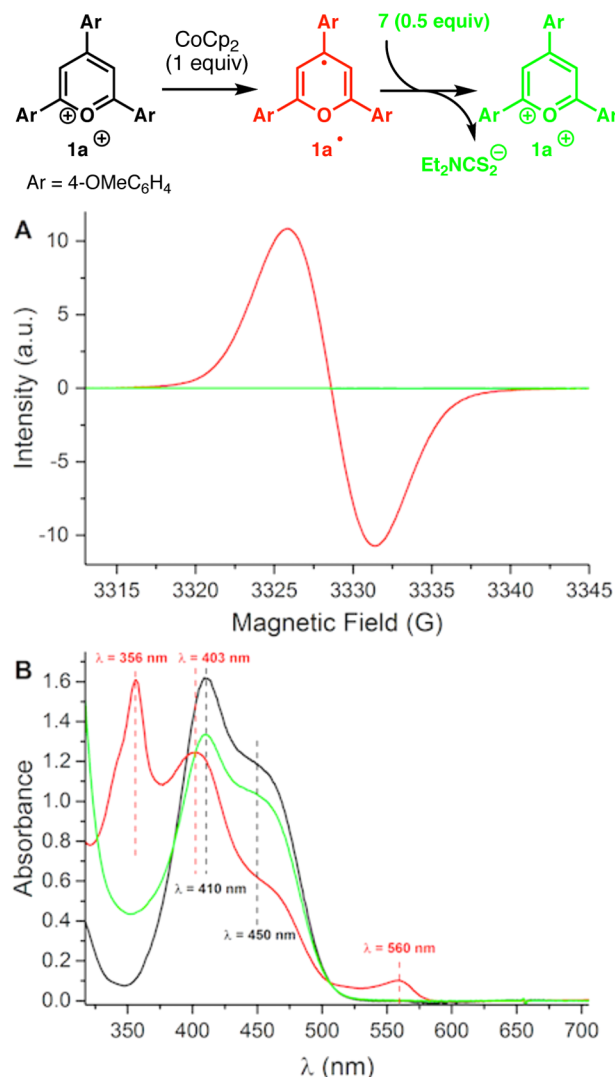


**Figure 15.** Reduction of 1a to 1a $^\bullet$  with CoCp<sub>2</sub>, followed by oxidation back to 1a with disulfide 7. (A) Electron spin resonance spectra of 1a (black underneath green curve), 1a $^\bullet$  after the addition of CoCp<sub>2</sub> (red), and 1a after the addition of 7 (green). (B) UV–visible spectra of 1a (black), 1a $^\bullet$  after the addition of CoCp<sub>2</sub> (red), and 1a after the addition of 7 (green). Characteristic absorption bands are indicated.

details). The spin concentration of this stable radical (lifetime >6 h) was estimated to be 250  $\mu$ M under these conditions. The addition of an excess of thiuram disulfide 7 resulted in an instantaneous depletion of the signal to a spin concentration of approximately 0.8  $\mu$ M (Figure 15A). This change indicated a SET from 1a $^\bullet$  to disulfide 7. The reduction of 7 concomitantly regenerates PC 1a, as shown on the UV–visible spectra (Figure 15B) and produces the dithiocarbamate anion likely responsible for capping the chain end and thus deactivating chain growth. In the polymerization process itself, this SET event likely happens with either 7 or the dithiocarbamate radical, which are postulated to be in equilibrium (Figure 13B).

Notably, the addition of CTA 2a to radical 1a $^\bullet$  generated by cobaltocene reduction resulted in no changes in the ESR and UV–visible spectra (Figure S26). This result corroborates the finding that the CTA does not interact with the reduced PC.



## CONCLUSION

Using various spectroscopic techniques, we gained intimate knowledge of each elementary step in a novel cationic polymerization of vinyl ethers regulated by visible light. Fine-tuning of the electronic structure of both the PC and the CTA unveiled a number of factors that govern the rate of polymerization as well as the prerequisites for a well-behaved living process: while more oxidizing pyrylium salts generally engender higher polymerization rates, quantum yields of fluorescence and the solubility profile also play a role in the activity of the PCs. Interestingly, no other family of PCs has proven competent for the photocontrolled polymerization of vinyl ethers yet. CTAs synthesized from a vinyl ether derivative and containing an electron-rich heteroatom appended to the dithiocarboxylic core delivered the best control over chain growth.

Time-resolved photoluminescence and ESR spectroscopy revealed single-electron transfers from excited PCs **1a\*** and **1b\*** to CTA **2a** and monomer **3a**. Oxidation of **3a** by PCs is responsible for the uncontrolled background polymerization. Comparison of bimolecular quenching constants and behaviors during cyclic voltammetry of **2a** and **3a**, however, suggests that oxidation of **2a** is more facile than that of **3a**, and that a second electron transfer from oxidized **3a** to **2a** might prevent the background polymerization. Moreover, polymerization of **3a** can be mediated by **2a** at a voltage lower than the onset of oxidation of **3a**, which indicates that the direct oxidation of **2a** by **1\*** is the major contributor to the activation step. Finally, the formation of a donor–acceptor complex between monomer and PC in the ground state was uncovered by meticulous ESR and UV–visible spectroscopic analyses of a mixture of **3a** and PCs **1a** and **1b**. Such complexes presumably play a key role in the activation step. Isolation of thiuram disulfide **7** supports a mesolytic cleavage pathway following oxidation of the CTA. In the reaction conditions, **7** is in equilibrium with the radical dithiocarbamate species arising from homolytic breaking of the disulfide bond. Determination of the quantum yields of polymerization for various PCs, as well as on/off experiments, substantiate the existence of a degenerative chain transfer mechanism. This RAFT-type equilibrium is likely pivotal in the obtention of polymers with predictable  $M_n$ 's and narrow  $D$ 's. Last, chain end deactivation and PC regeneration via electron transfer between **1a\*** and **7** were corroborated by ESR and UV–visible spectroscopies.

We are confident that the results of this study will serve as a starting point for explorations of similar photoredox-catalyzed polymerizations and that our findings will prove critical in the eventual adoption of this system in complex practical settings.

## ASSOCIATED CONTENT

### Supporting Information

The Supporting Information is available free of charge on the ACS Publications website at DOI: 10.1021/jacs.7b09539.

General experimental considerations, experimental procedures, and additional supporting data (PDF)

## AUTHOR INFORMATION

### Corresponding Author

\*bpf46@cornell.edu

ORCID

Timothée Chauviré: 0000-0002-9466-4785

Héctor D. Abruña: 0000-0002-3948-356X

Jack H. Freed: 0000-0003-4288-2585

Brett P. Fors: 0000-0002-2222-3825

### Notes

The authors declare no competing financial interest.

## ACKNOWLEDGMENTS

This work was supported by Cornell University, made use of the NMR facility at Cornell University, and was supported in part by the National Science Foundation under Award CHE-1531632. It also made use of the National Biomedical Research Center for Advanced ESR Technology (ACERT) and was supported by the National Institute of General Medical Sciences of the National Institutes of Health under Award Number P41GM103521. B.P.F. thanks 3M for a Nontenured Faculty Award.

## REFERENCES

- (1) (a) Chen, M.; Zhong, M.; Johnson, J. A. *Chem. Rev.* **2016**, *116*, 10167. (b) Corrigan, N.; Shanmugam, S.; Xu, J.; Boyer, C. *Chem. Soc. Rev.* **2016**, *45*, 6165. (c) Trotta, J. T.; Fors, B. P. *Synlett* **2016**, *27*, 702. (d) Dadashi-Silab, S.; Doran, S.; Yagci, Y. *Chem. Rev.* **2016**, *116*, 10212. (e) Pan, X.; Tasdelen, M. A.; Laun, J.; Junkers, T.; Yagci, Y.; Matyjaszewski, K. *Prog. Polym. Sci.* **2016**, *62*, 73. (f) Michaudel, Q.; Kottisch, V.; Fors, B. P. *Angew. Chem., Int. Ed.* **2017**, *56*, 2. (g) Shanmugam, S.; Xu, J.; Boyer, C. *Macromol. Rapid Commun.* **2017**, *38*, 1700143. (h) Ciftci, M.; Yilmaz, G.; Yagci, Y. *J. Photopolym. Sci. Technol.* **2017**, *30*, 385.
- (2) For selected examples, see: (a) Koumura, K.; Satoh, K.; Kamigaito, M. *Macromolecules* **2008**, *41*, 7359. (b) Kwak, Y.; Matyjaszewski, K. *Macromolecules* **2010**, *43*, 5180. (c) Tasdelen, M. A.; Uygun, M.; Yagci, Y. *Macromol. Chem. Phys.* **2010**, *211*, 2271. (d) Fors, B. P.; Hawker, C. J. *Angew. Chem., Int. Ed.* **2012**, *51*, 8850. (e) Konkolewicz, D.; Schroder, K.; Buback, J.; Bernhard, S.; Matyjaszewski, K. *ACS Macro Lett.* **2012**, *1*, 1219. (f) Ciftci, M.; Tasdelen, M. A.; Li, W.; Matyjaszewski, K.; Yagci, Y. *Macromolecules* **2013**, *46*, 9537. (g) Anastasaki, A.; Nikolaou, V.; Zhang, Q.; Burns, J.; Samanta, S. R.; Waldron, C.; Haddleton, A. J.; McHale, R.; Fox, D.; Percec, V.; Wilson, P.; Haddleton, D. M. *J. Am. Chem. Soc.* **2014**, *136*, 1141. (h) Treat, N. J.; Sprafke, H.; Kramer, J. W.; Clark, P. G.; Barton, B. E.; Read de Alaniz, J.; Fors, B. P.; Hawker, C. J. *J. Am. Chem. Soc.* **2014**, *136*, 16096. (i) Anastasaki, A.; Nikolaou, V.; Simula, A.; Godfrey, J.; Li, M.; Nurumbetov, G.; Wilson, P.; Haddleton, D. M. *Macromolecules* **2014**, *47*, 3852. (j) Ribelli, T. G.; Konkolewicz, D.; Bernhard, S.; Matyjaszewski, K. *J. Am. Chem. Soc.* **2014**, *136*, 13303. (k) Pan, X.; Malhotra, N.; Simakova, A.; Wang, Z.; Konkolewicz, D.; Matyjaszewski, K. *J. Am. Chem. Soc.* **2015**, *137*, 15430. (l) Melker, A.; Fors, B. P.; Hawker, C. J.; Poelma, J. E. *J. Polym. Sci., Part A: Polym. Chem.* **2015**, *53*, 2693. (m) Frick, E.; Anastasaki, A.; Haddleton, D. M.; Barner-Kowollik, C. *J. Am. Chem. Soc.* **2015**, *137*, 6889. (n) Anastasaki, A.; Nikolaou, V.; Brandford-Adams, F.; Nurumbetov, G.; Zhang, Q.; Clarkson, G. J.; Fox, D. J.; Wilson, P.; Kempe, K.; Haddleton, D. M. *Chem. Commun.* **2015**, *51*, 5626. (o) Pan, X.; Fang, C.; Fantin, M.; Malhotra, N.; So, W. Y.; Peteanu, L. A.; Isse, A. A.; Gennaro, A.; Liu, P.; Matyjaszewski, K. *J. Am. Chem. Soc.* **2016**, *138*, 2411. (p) Jones, G. R.; Whitfield, R.; Anastasaki, A.; Haddleton, D. M. *J. Am. Chem. Soc.* **2016**, *138*, 7346. (q) Nikolaou, V.; Anastasaki, A.; Brandford-Adams, F.; Whitfield, R.; Jones, G. R.; Nurumbetov, G.; Haddleton, D. M. *Polym. Chem.* **2016**, *7*, 191. (r) Theriot, J. C.; Lim, C.-H.; Yang, H.; Ryan, M. D.; Musgrave, C. B.; Miyake, G. M. *Science* **2016**, *352*, 1082. (s) Pearson, R. M.; Lim, C.-H.; McCarthy, B. G.; Musgrave, C. B.; Miyake, G. M. *J. Am. Chem. Soc.* **2016**, *138*, 11399. (t) Ciftci, M.; Yoshikawa, Y.; Yagci, Y. *Angew. Chem., Int. Ed.* **2017**, *56*, 519. (u) Ramsey, B. L.; Pearson, R. M.; Beck, L. R.; Miyake, G. M. *Macromolecules* **2017**, *50*, 2668. (v) Zhu, C.; Schneider, E. K.; Nikolaou, V.; Klein, T.; Li, J.; Davis, T. P.; Whittaker, M. R.; Wilson, P.; Kempe, K.; Velkov, T.; Haddleton, D. M. *Bioconjugate Chem.* **2017**, *28*, 1916. (w) Dadashi-Silab, S.; Pan, X.; Matyjaszewski, K. *Chem. - Eur. J.* **2017**, *23*, 5972. (x) Pan, X.; Lathwal, S.; Mack, S.; Yan, J.; Das, S. R.; Matyjaszewski, K. *Angew. Chem., Int. Ed.* **2017**, *56*, 2740.



- (y) Lim, C.-H.; Ryan, M. D.; McCarthy, B. G.; Theriot, J. C.; Sartor, S. M.; Damrauer, N. H.; Musgrave, C. B.; Miyake, G. M. *J. Am. Chem. Soc.* **2017**, *139*, 348.
- (3) For selected examples, see: (a) Yamago, S.; Ukai, Y.; Matsumoto, A.; Nakamura, Y. *J. Am. Chem. Soc.* **2009**, *131*, 2100. (b) Nakamura, Y.; Arima, T.; Tomita, S.; Yamago, S. *J. Am. Chem. Soc.* **2012**, *134*, 5536.
- (4) For selected examples, see: (a) Xu, J.; Jung, K.; Atme, A.; Shanmugam, S.; Boyer, C. *J. Am. Chem. Soc.* **2014**, *136*, 5508. (b) Chen, M.; MacLeod, M. J.; Johnson, J. A. *ACS Macro Lett.* **2015**, *4*, 566. (c) Shanmugam, S.; Xu, J.; Boyer, C. *J. Am. Chem. Soc.* **2015**, *137*, 9174. (d) Xu, J.; Shanmugam, S.; Duong, H. T.; Boyer, C. *Polym. Chem.* **2015**, *6*, 5615. (e) Shanmugam, S.; Xu, J.; Boyer, C. *Chem. Sci.* **2015**, *6*, 1341. (f) Shanmugam, S.; Boyer, C. *J. Am. Chem. Soc.* **2015**, *137*, 9988. (g) Shanmugam, S.; Xu, J.; Boyer, C. *Angew. Chem., Int. Ed.* **2016**, *55*, 1036. (h) Xu, J.; Shanmugam, S.; Fu, C.; Aguey-Zinsou, K.; Boyer, C. *J. Am. Chem. Soc.* **2016**, *138*, 3094. (i) Shanmugam, S.; Xu, J.; Boyer, C. *Polym. Chem.* **2016**, *7*, 6437. (j) Fu, C.; Xu, J.; Boyer, C. *Chem. Commun.* **2016**, *52*, 7126. (k) Yeow, J.; Shanmugam, S.; Corrigan, N.; Kuchel, R. P.; Xu, J.; Boyer, C. *Macromolecules* **2016**, *49*, 7277. (l) Corrigan, N.; Xu, J.; Boyer, C. *Macromolecules* **2016**, *49*, 3274. (m) Tucker, B. S.; Coughlin, M. L.; Figg, C. A.; Sumerlin, B. S. *ACS Macro Lett.* **2017**, *6*, 452. (n) Chen, M.; Deng, S.; Gu, Y.; Lin, J.; MacLeod, M. J.; Johnson, J. A. *J. Am. Chem. Soc.* **2017**, *139*, 2257. (o) Lee, I.-H.; Discekici, E. H.; Anastasaki, A.; Read de Alaniz, J.; Hawker, C. J. *Polym. Chem.* **2017**, *8*, 3351. Ng, G.; Yeow, J.; Xu, J.; Boyer, C. *Polym. Chem.* **2017**, *8*, 2841.
- (5) (a) Poelma, J. E.; Fors, B. P.; Meyers, G. F.; Kramer, J. W.; Hawker, C. J. *Angew. Chem., Int. Ed.* **2013**, *52*, 6844. (b) Vorobii, M.; de los Santos Pereira, A.; Pop-Georgievski, O.; Kostina, N. Y.; Rodriguez-Emmenegger, C.; Percec, V. *Polym. Chem.* **2015**, *6*, 4210. (c) Pester, C. W.; Poelma, J. E.; Narupai, B.; Patel, S. N.; Su, G. M.; Mates, T. E.; Luo, Y.; Ober, C. K.; Hawker, C. J.; Kramer, E. J. *J. Polym. Sci., Part A: Polym. Chem.* **2016**, *54*, 253. (d) Discekici, E. H.; Pester, C. W.; Treat, N. J.; Lawrence, J.; Mattson, K. M.; Narupai, B.; Toumayan, E. P.; Luo, Y.; McGrath, A. J.; Clark, P. G.; Read de Alaniz, J.; Hawker, C. J. *ACS Macro Lett.* **2016**, *5*, 258. (e) Yan, J.; Pan, X.; Schmitt, M.; Wang, Z.; Bockstaller, M. R.; Matyjaszewski, K. *ACS Macro Lett.* **2016**, *5*, 661. (f) Pester, C. W.; Narupai, B.; Mattson, K. M.; Bothman, D. P.; Klinger, D.; Lee, K. W.; Discekici, E. H.; Hawker, C. J. *Adv. Mater.* **2016**, *28*, 9292. (g) Narupai, B.; Poelma, J. E.; Pester, C. W.; McGrath, A. J.; Toumayan, E. P.; Luo, Y.; Kramer, J. W.; Clark, P. G.; Ray, P. C.; Hawker, C. J. *J. Polym. Sci., Part A: Polym. Chem.* **2016**, *54*, 2276. (h) Yang, Y.; Liu, X.; Ye, G.; Zhu, S.; Wang, Z.; Huo, X.; Matyjaszewski, K.; Lu, Y.; Chen, J. *ACS Appl. Mater. Interfaces* **2017**, *9*, 13637. (i) Page, Z. A.; Narupai, B.; Pester, C. W.; Zerdan, R. B.; Sokolov, A.; Laitar, D. S.; Mukhopadhyay, S.; Sprague, S.; McGrath, A. J.; Kramer, J. W.; Trefonas, P.; Hawker, C. J. *ACS Cent. Sci.* **2017**, *3*, 654.
- (6) (a) Xu, J.; Fu, C.; Shanmugam, S.; Hawker, C. J.; Moad, G.; Boyer, C. *Angew. Chem.* **2017**, *129*, 8496. (b) Xu, J.; Shanmugam, S.; Fu, C.; Aguey-Zinsou, K.; Boyer, C. *J. Am. Chem. Soc.* **2016**, *138*, 3094. (c) Fu, C.; Huang, Z.; Hawker, C. J.; Moad, G.; Xu, J.; Boyer, C. *Polym. Chem.* **2017**, *8*, 4637.
- (7) Kottisch, V.; Michaudel, Q.; Fors, B. P. *J. Am. Chem. Soc.* **2016**, *138*, 15535.
- (8) Romero, N. A.; Nicewicz, D. A. *Chem. Rev.* **2016**, *116*, 10075.
- (9) Pascual, L. M. M.; Dunford, D. G.; Goetz, A. E.; Ogawa, K. A.; Boydston, A. J. *Synlett* **2016**, *27*, 759.
- (10) Martiny, M.; Steckhan, E.; Esch, T. *Chem. Ber.* **1993**, *126*, 1671.
- (11) Miranda, M. A.; Izquierdo, M. A.; Galindo, F. *J. Org. Chem.* **2002**, *67*, 4138.
- (12) Romero, N. A.; Nicewicz, D. A. *J. Am. Chem. Soc.* **2014**, *136*, 17024.
- (13) Prier, C. K.; Rankic, D. A.; MacMillan, D. W. C. *Chem. Rev.* **2013**, *113*, 5322.
- (14) Kajouji, S.; Marcélis, L.; Lemaire, V.; Beljonne, D.; Moucheron, C. *Dalton Trans.* **2017**, *46*, 6623.
- (15) Ross, H. B.; Boldaji, M. D.; Rillema, P.; Blanton, C. B.; White, R. P. *Inorg. Chem.* **1989**, *28*, 1013.
- (16) Lowry, M. S.; Goldsmith, J. I.; Slinker, J. D.; Rohl, R.; Pascal, R. A., Jr.; Malliaras, G. G.; Bernhard, S. *Chem. Mater.* **2005**, *17*, 5712.
- (17) Zivic, N.; Bouzrati-Zerelli, M.; Kermagoret, A.; Dumur, F.; Fouassier, J.-P.; Gimes, D.; Lalevée, J. *ChemCatChem* **2016**, *8*, 1617.
- (18) Jockusch, S.; Yagci, Y. *Polym. Chem.* **2016**, *7*, 6039.
- (19) (a) Aoshima, H.; Uchiyama, M.; Satoh, K.; Kamigaito, M. *Angew. Chem., Int. Ed.* **2014**, *53*, 10932. (b) Uchiyama, M.; Satoh, K.; Kamigaito, M. *Angew. Chem., Int. Ed.* **2015**, *54*, 1924.
- (20) All solvents were dried through activated alumina columns or distillation, and degassed before use; see SI for more details.
- (21) Deffieux, A.; Young, J. A.; Hsieh, W. C.; Squire, D. R.; Stannett, V. *Polymer* **1983**, *24*, 573.
- (22) Lakowicz, J. R. *Principles of Fluorescence Spectroscopy*, 3rd ed.; Springer: New York, 2006.
- (23) Uncontrolled cationic polymerizations of vinyl ethers via anodic oxidation have been reported. See: (a) Mengoli, G.; Vidotto, G. *Makromol. Chem.* **1970**, *139*, 293. (b) Breitenbach, J. W.; Sommer, F.; Unger, G. *Monatsh. Chem.* **1976**, *107*, 359. (c) Nuyken, O.; Braun, H.; Crivello, J. In *Handbook of Polymer Synthesis*, 2nd ed.; Kricheldorf, H. R., Nuyken, O., Swift, G., Eds.; Marcel Dekker: New York, 2004.
- (24) El-Roz, M.; Lalevée, J.; Morlet-Savary, F.; Allonas, X.; Fouassier, J. P. *J. Polym. Sci., Part A: Polym. Chem.* **2008**, *46*, 7369.
- (25) (a) Degani, I.; Lunazzi, L.; Pedulli, G. F. *Mol. Phys.* **1968**, *14*, 217. (b) Niizuma, S.; Sato, N.; Kawata, H.; Suzuki, Y.; Toda, T.; Kokubun, H. *Bull. Chem. Soc. Jpn.* **1985**, *58*, 2600.
- (26) Kawata, H.; Niizuma, S. *Bull. Chem. Soc. Jpn.* **1989**, *62*, 2279.
- (27) Neither decreasing the concentration of **3a** (ESR signal became too weak to be resolved) nor increasing the temperature in the ESR cavity (the radical became unstable above 303 K) overcame the broadening issue.
- (28) (a) Currin, J. D. *Phys. Rev.* **1962**, *126*, 1995. (b) Bales, B. L.; Peric, M.; Dragutan, I. *J. Phys. Chem. A* **2003**, *107*, 9086.
- (29) Poole, C. P.; Farach, H. A. *Bull. Magn. Reson.* **1979**, *1*, 162.
- (30) Benesi, H. A.; Hildebrand, J. H. *J. Am. Chem. Soc.* **1949**, *71*, 2703.
- (31) Two independent, overlapping spin systems could also explain the spectra of Figure 11.
- (32) Sugihara, S.; Kawamoto, Y.; Maeda, Y. *Macromolecules* **2016**, *49*, 1563.
- (33) Kottisch, V.; Michaudel, Q.; Fors, B. P. *J. Am. Chem. Soc.* **2017**, *139*, 10665.
- (34) (a) Liang, F.; Tan, J.; Piao, C.; Liu, Q. *Synthesis* **2008**, *2008*, 3579. (b) Kapanda, C. N.; Muccioli, G. G.; Labar, G.; Poupaert, J. H.; Lambert, D. M. *J. Med. Chem.* **2009**, *52*, 7310.
- (35) (a) Schubart, R. Dithiocarbamic Acid and Derivatives. In *Ullmann's Encyclopedia of Industrial Chemistry*; Wiley-VCH: Weinheim, 2002. (b) Otsu, T. *J. Polym. Sci., Part A: Polym. Chem.* **2000**, *38*, 2121.
- (36) Uchiyama, M.; Satoh, K.; Kamigaito, M. *Macromolecules* **2015**, *48*, 5533.
- (37) Sugihara, S.; Konegawa, N.; Maeda, Y. *Macromolecules* **2015**, *48*, 5120.
- (38) (a) Demas, J. N.; Bowman, W. D.; Zalewski, E. F.; Velapoldi, R. A. *J. Phys. Chem.* **1981**, *85*, 2766. (b) Kuhn, H. J.; Braslavsky, S. E.; Schmidt, R. *Pure Appl. Chem.* **2004**, *76*, 2105.
- (39) Decker, C.; Moussa, K. *J. Polym. Sci., Part A: Polym. Chem.* **1990**, *28*, 3429.
- (40) Nichols, P. J.; Grant, M. W. *Aust. J. Chem.* **1982**, *35*, 2455.
- (41)  $E_{1/2} = -0.91$  V vs SCE; see: Montalti, M.; Credi, A.; Prodi, L.; Gandolfi, M. T. *Handbook of Photochemistry*, 3rd ed.; CRC Press: 2006.